REPORT DOCUMENTATION PAGE

Form Approved OMB NO. 0704-0188

1. REPORT DATE (DD-MM-YYYY)	2. REPORT TYPE	3. DATES COVERED (From - To)
	Technical Report	-

4. TITLE AND SUBTITLE
Mitigating Stress Waves Using Nanofoams and Nanohoneycombs

5a. CONTRACT NUMBER
W911NF-12-1-0011

5b. GRANT NUMBER

5c. PROGRAM ELEMENT NUMBER
611102

6. AUTHORS
Dr. Yu Qiao

5d. PROJECT NUMBER

5e. TASK NUMBER

5f. WORK UNIT NUMBER

7. PERFORMING ORGANIZATION NAMES AND ADDRESSES
University of California - San Diego
9500 Gilman Drive
MC 0934
La Jolla, CA 92093 -0934

8. PERFORMING ORGANIZATION REPORT NUMBER

9. SPONSORING/MONITORING AGENCY NAME(S) AND ADDRESS (ES)
U.S. Army Research Office
P.O. Box 12211
Research Triangle Park, NC 27709-2211

10. SPONSOR/MONITOR'S ACRONYM(S)
ARO

11. SPONSOR/MONITOR'S REPORT NUMBER(S)
58458-MS.2

12. DISTRIBUTION AVAILIBILITY STATEMENT
Approved for public release; distribution is unlimited.

13. SUPPLEMENTARY NOTES
The views, opinions and/or findings contained in this report are those of the author(s) and should not contrued as an official Department of the Army position, policy or decision, unless so designated by other documentation.

14. ABSTRACT
(1) In the past 10 months, we conducted quasi-static shear tests and SHB dynamic tests on single-parameter silica foam samples. The testing data showed consistent correlation between the cell size and the transmitted pulse pressure and energy: Reducing cell size to below 100-200 nm has a significant beneficial effect on promoting energy absorption.

To achieve the above result, we also

15. SUBJECT TERMS
Stress wave, Nanofoams, Energy absorption, shear band

16. SECURITY CLASSIFICATION OF:			17. LIMITATION OF ABSTRACT	15. NUMBER OF PAGES	19a. NAME OF RESPONSIBLE PERSON
a. REPORT	b. ABSTRACT	c. THIS PAGE			Yu Qiao
UU	UU	UU	UU		19b. TELEPHONE NUMBER 858-534-3388

Report Title

Mitigating Stress Waves Using Nanofoams and Nanohoneycombs

ABSTRACT

(1) In the past 10 months, we conducted quasi-static shear tests and SHB dynamic tests on single-parameter silica foam samples. The testing data showed consistent correlation between the cell size and the transmitted pulse pressure and energy: Reducing cell size to below 100-200 nm has a significant beneficial effect on promoting energy absorption.

To achieve the above result, we also

(2) Further improved the SHB testing system, and developed single-pulse momentum trapper;

(3) Developed a quantitative SEM image analysis technique to precisely identify shear bands, compression zones, and undamaged zones in tested samples.

(4) Synthesized two-parameter silica foam samples, with the cell size ranging from tens of nm to a few ?m and the porosity ranging from ~60% to ~80%.

(5) Performed quasi-static shear tests and SHB dynamic tests on two-parameter silica foam samples. The testing data, although interesting, are non-conclusive, as the influences of cell size and porosity cannot be separately analyzed.

(6) Developed new approaches and synthesized one-parameter silica foam samples, which had nearly identical porosity but different cell sizes from tens of nm to more than 1 ?m.

(7) Quantitative SEM image analysis of one-parameter samples is being performed.

INTERIM PROGRESS REPORT

Date: April 16th, 2014

Period of Performance of this Report: August 1st, 2013 – April 14th, 2014

Project Title: Mitigating Stress Waves Using Nanofoams and Nanohoneycombs

Grant No.: W911NF-12-1-0011

Program Manager: Dr. David M. Stepp

PI: Professor Yu Qiao
Department of Structural Engineering
University of California – San Diego
9500 Gilman Dr. MC 0085, La Jolla, CA 92093-0085
Phone: 858-534-3388
Email: yqiao@ucsd.edu

Other Personnel Involved in the Project:

Dr. Weiyi Lu, Postdoctoral Researcher

Mr. Cang Zhao, Graduate Student Researcher

SUMMARY OF PREVIOUS ACHIEVEMENTS

- Modified the Split Hopkinson Bar (SHB) system, and accurately measured transmitted pulses;
- Verified the effectiveness of the Shear Promotion Holder (SPH) technique, and enhanced it to the Improved Shear Promotion Holder (ISPH) technique;
- Enhanced the processing capacity and the quality of silica nanofoams;
- Performed dynamic tests on silica nanofoam samples, and observed shear bands.

SUMMARY OF NEW ACHIEVEMENTS

- In the past 10 months, we conducted quasi-static shear tests and SHB dynamic tests on single-parameter silica foam samples. The testing data showed consistent correlation between the cell size and the transmitted pulse pressure and energy: Reducing cell size to below 100-200 nm has a significant beneficial effect on promoting energy absorption. The detailed results are presented in **Section 2.4** below.

To achieve the above result, we

- Further improved the SHB testing system, and developed single-pulse momentum trapper;
- Developed a quantitative SEM image analysis technique to precisely identify shear bands, compression zones, and undamaged zones in tested samples.
- Synthesized two-parameter silica foam samples, with the cell size ranging from tens of nm to a few μm and the porosity ranging from ~60% to ~80%.
- Performed quasi-static shear tests and SHB dynamic tests on two-parameter silica foam samples. The testing data, although interesting, are non-conclusive, as the influences of cell size and porosity cannot be separately analyzed.
- Developed new approaches and synthesized one-parameter silica foam samples, which had nearly identical porosity but different cell sizes from tens of nm to more than 1 μm.
- Quantitative SEM image analysis of one-parameter samples is being performed.

In the following sections, we present our work in chronological order.

1. TWO-PARAMETER STUDY ON SILICA NANOFOAMS

1.1 Preparation and Characterization of Silica Nanofoams

Following the work in the last period of performance, we performed a systematic study on silica nanofoam samples with the cell sizes ranging from tens of nm to a few microns.

1.1.1 Silica Nanofoams

Silica nanofoam was prepared through Shoup method.[1] As shown in Figure 1.1.1, potassium silicate solution was mixed with colloidal silica at various ratios ranging from 1:99 to 45:55, so as to control the pore size. Using a plastic vial (Figure 1.1.2) as the curing mold, large-sized, disk-shaped samples were successfully synthesized.

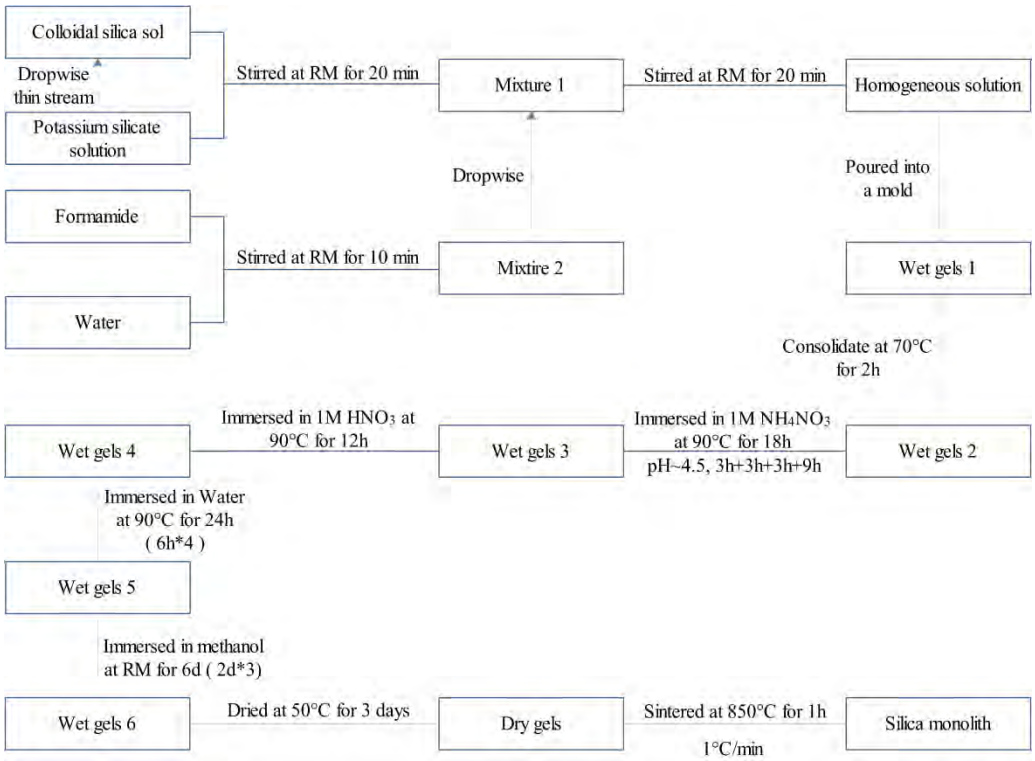

Fig.1.1.1 Flow chart of silica nanofoam processing

After being treated at 850 C for 1 hour, the density of the samples was measured, as shown in Table 1.1.1. As the reference density of solid amorphous silica was taken as 2.2 g/cm^3, the relative density and the porosity of the silica nanofoam were calculated, which varied in the range of 0.14-0.24 and 76%-86%, respectively.

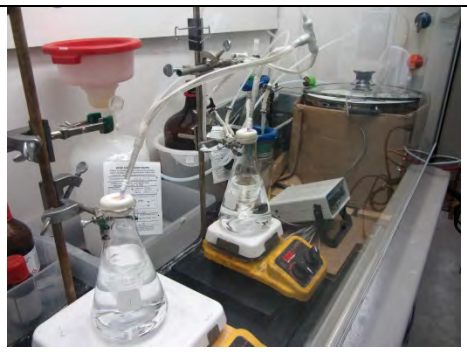

(a) Sol-gel synthesis

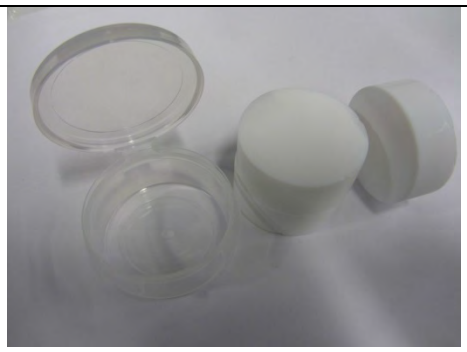

(b) Silica nanfoam samples

Fig.1.1.2 Experimental setups

Table 1.1.1 Density and porosity of silica foam

Sample No.	Composition ratio	Sample diameter (mm)	Relative density (g/cm^3)	Porosity
1	3 : 97	19.43	0.523	76.2%
2	5 : 95	20.00	0.465	78.8%
3	10 : 90	20.82	0.442	79.9%
4	15 : 85	21.72	0.395	82.1%
5	17 : 83	22.09	0.385	82.5%
6	19 : 81	22.39	0.376	82.9%
7	23 : 77	22.98	0.356	83.8%
8	25 : 75	23.27	0.350	84.1%
9	30 : 70	23.88	0.330	85.0%
10	40 : 60	24.67	0.317	85.6%

The specific pore volume was measured by mercury porosimetry and the cell size was calculated from the well-established Washburn method (Fig.1.1.3). The results were listed in Table 1.1.2. Scanning electron microscope (SEM) images show the microstructures of the silica nanofoams (Figure 1.1.4). It can be seen that in all the samples, the cell configurations are quite similar.

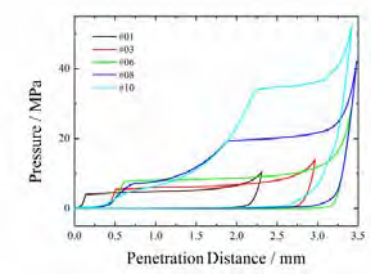

(a) Mercury penetration porosimetry. The loading rate is 0.1 mm/min.

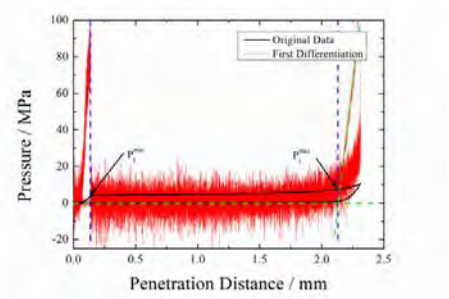

(b) Definition of the cell size range

Fig.1.1.3 Mercury porosimetry curves.

Table 1.1.2 The cell size ranges of the silica nanofoams

Sample No.	Porosity	Cell Size / nm		Average Cell Size / nm
		min	max	
1	76.2%	204	398	301
2	78.8%	166	303	235
3	79.9%	154	249	201
4	82.1%	118	221	170
5	82.5%	114	212	163
6	82.9%	109	195	152
7	83.8%	97	166	132
8	84.1%	80	97	88
9	85.0%	59	65	62
10	85.6%	40	44	42

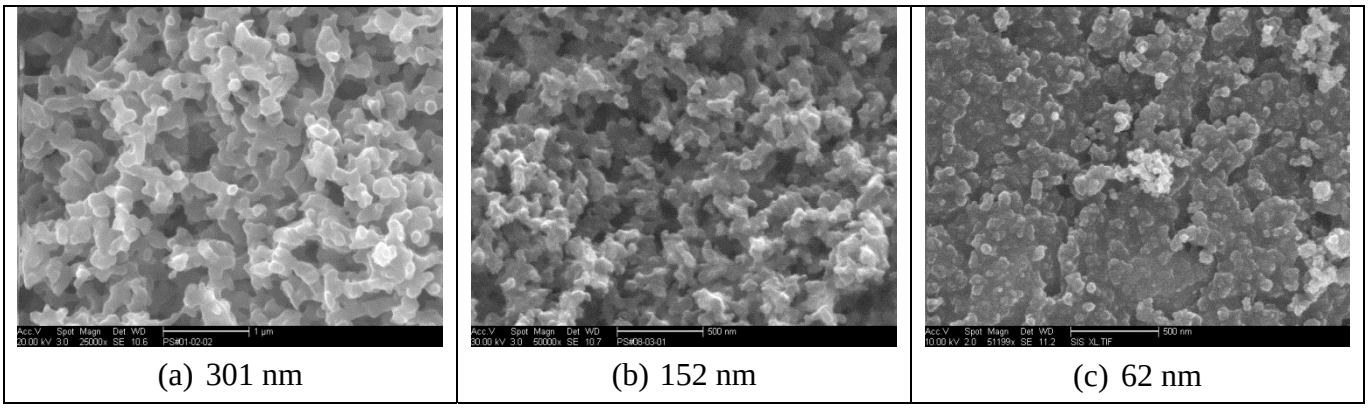

(a) 301 nm (b) 152 nm (c) 62 nm

Fig.1.1.4 SEM images of silica foam with average cell size less than 500 nm

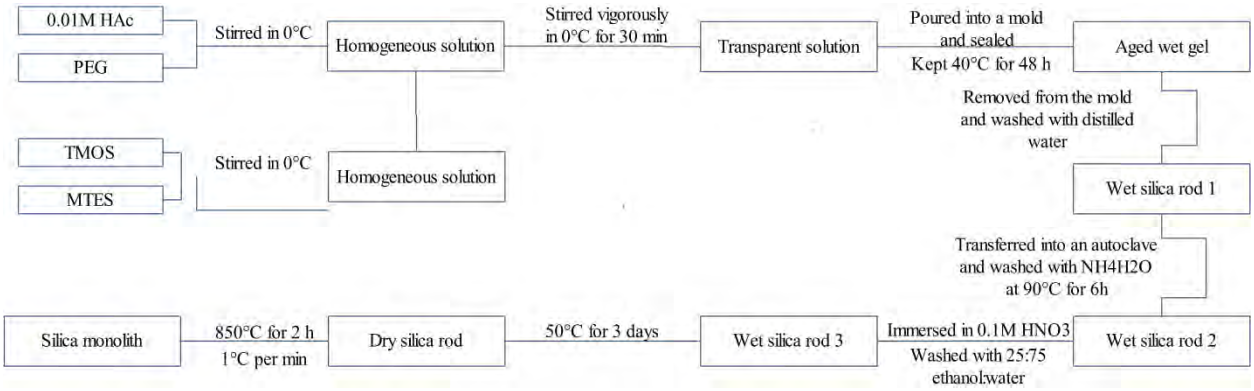

Fig.1.1.5 Flow chart of silica foam processing with average cell size about a few microns

1.1.2 Large-Celled Silica Foams

Large-celled silica foams were synthesized through the Nakanishi method. TMOS was added into 0.01 M acetic acid solution which had dissolved PEG with the molecular weight around

10,000. The cell size was adjusted by tailing the TMOS to PEG ratio. The flow chart is shown in Fig.1.1.5.

The density, the porosity, and the cell size distribution of the silica foams were characterized through mercury porosimetry. For the silica foam sample synthesized by 70.0 ml TMOS and 14.0 g PEG, the density was 0.263 g/cm^3, and the corresponding porosity was 88.1%. Figure 1.1.6 shows the typical cell structure.

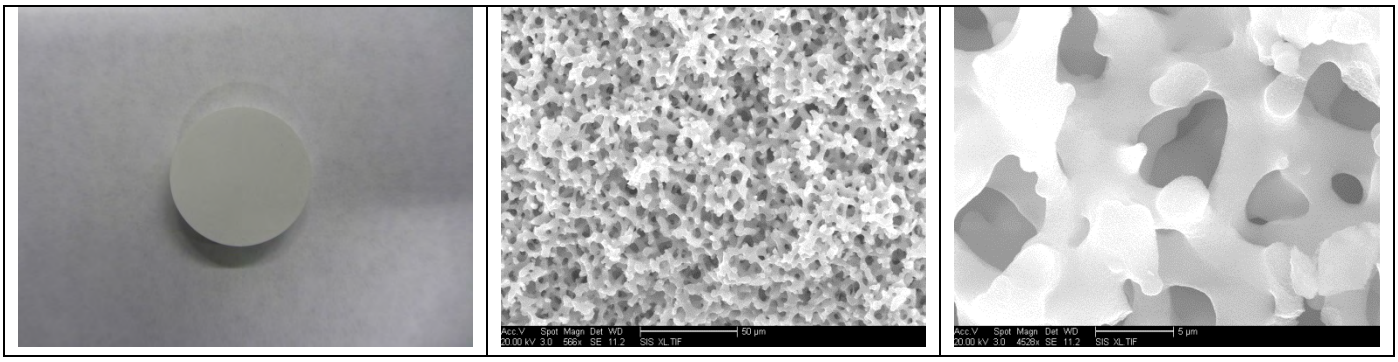

Fig.1.1.6 A photo and SEM images of a large-celled silica foam.

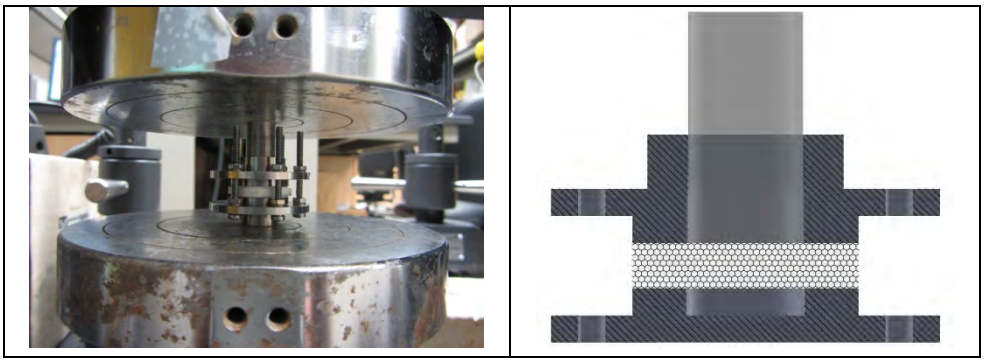

Fig.1.2.1 Quasi-Static shear test setup

1.2 Quasi-Static Shear Experiment

1.2.1 Experimental Setup

As depicted in Figure 1.2.1, forced-shear tests on silica foams were conducted by using an Instron type-5582 machine, with the loading rate of 0.01 mm/min. An improved shear promotion holder (ISPH) was employed to prevent bending of the disc sample, equipped with a silicone rubber ring providing sufficient lateral confinement.

1.2.2 Results and Analysis

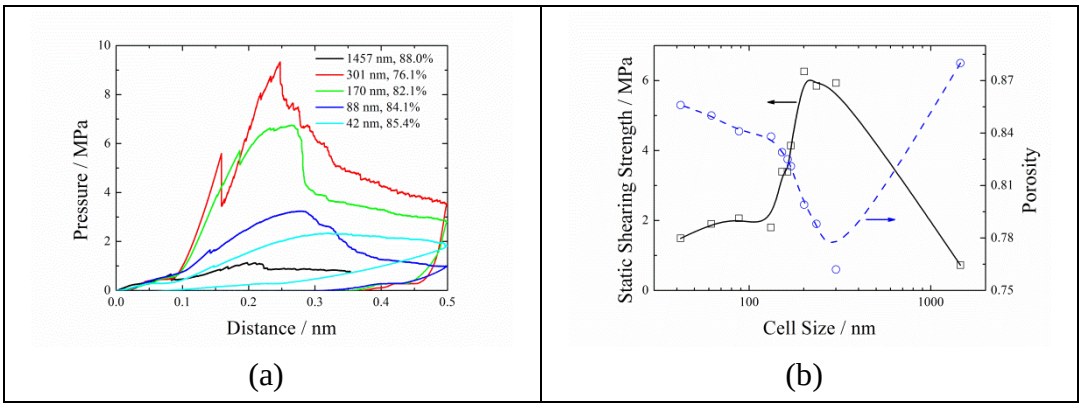

(a) (b)

Fig.1.2.2 Results of quasi-static shear tests
(Sample thickness: 5.0 mm; Loading rate: 0.01 mm/min; Shear depth: 0.5 mm)

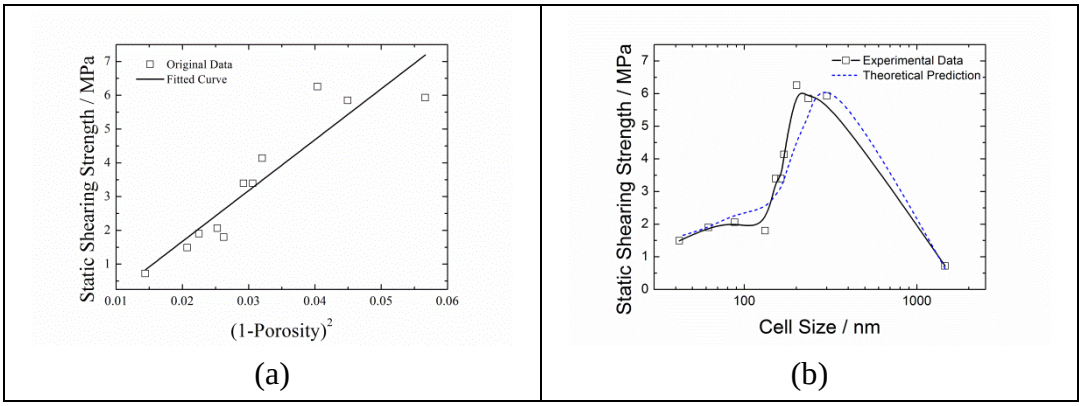

(a) (b)

Fig.1.2.3 Static shearing strength

The quasi-static shear strength of silica foam was calculated as

$$\tau_f = \frac{F}{A} = \frac{B_f \cdot A_b}{A} = \frac{B_f \cdot \pi D^2/4}{\pi D t} = \frac{B_f \cdot D}{4t}$$

where D is the diameter of the intrusion rod, P_f is the failure loading, and t is the sample thickness.

Figure 1.2.2(b) indicates that the silica foam samples with a lower porosity tend to have a higher quasi-static shear strength. Taken the sample with the porosity of 88.0% for example, the quasi-static shear strength is 0.72 MPa; while the sample with the porosity of 76.2% has a much higher shearing strength, nearly 6.0 MPa. That is, the quasi-static shear strength is highly sensitive to the porosity.

Consider a foam with open cells, the shear modulus is

$$G_{foam} = \frac{\tau}{\gamma} = G \cdot E_{solid} \left(\frac{\rho_{foam}}{\rho_{solid}}\right)^2 = G \cdot E_{solid} (1-\phi)^2$$

where C is a material constant, E_{Solid} is the Young's modulus of solid material, and Φ is the porosity. Assume that the failure strain is independent of the cell size. The shear strength can then be assessed as

$$\sigma_f = C \cdot E_{Solid} \cdot \varepsilon_f \cdot (1-\phi)^2 = C^* \cdot (1-\phi)^2$$

where C^* is another material constant. Through data fitting, the value of C^* was obtained as 151 ± 21 MPa for the silica nanoforms under investigation (Fig.1.2.3a). The theoretical result fits with the testing data quite well, as shown in Fig.1.2.3(b): The quasi-static strength of a foam is heavily dependent on its porosity, while relatively unrelated to the cell size.

1.3 SHPB Testing on Silica Foams

1.3.1 Improvement in Experimental Setup

SHPB system was used to conduct dynamic tests on the silica foam samples. Improved shear promotion holder (ISPH) was employed to promote shear band formation. The details of the testing system and method have been discussed in the last report.

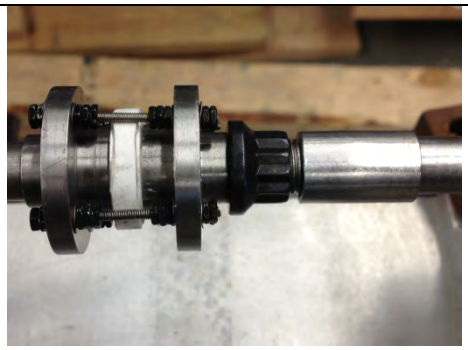

(a) Old version

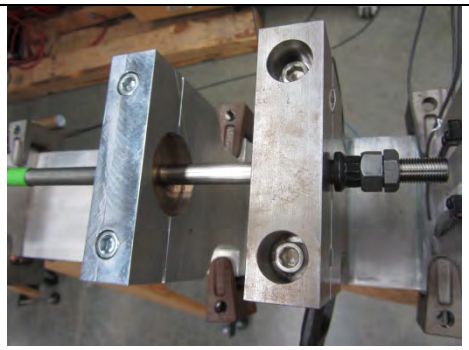

(b) Updated version

Fig.1.3.1 The momentum trapper

A momentum trapper (MT) was developed to prevent repeated dynamic loading on the testing sample; that is, after the first stress wave pulse passes through the sample, the incident bar is immediately separately from the sample, so that the reflected waves would not affect the sample behaviors. The main purpose of MT is to preserve the foam sample; otherwise it may undergo intensive cracking and detailed analysis of the shear banding process becomes impossible. Compared with the earlier version, shown in Figure 1.3.1(a), the improved MT, which was placed directly at the front of the incident bar, also simplifies the interface between the incident bar and the sample, minimizing the possible compression damage caused by the front part of the ISPH. Sample handling and mounting is also easier.

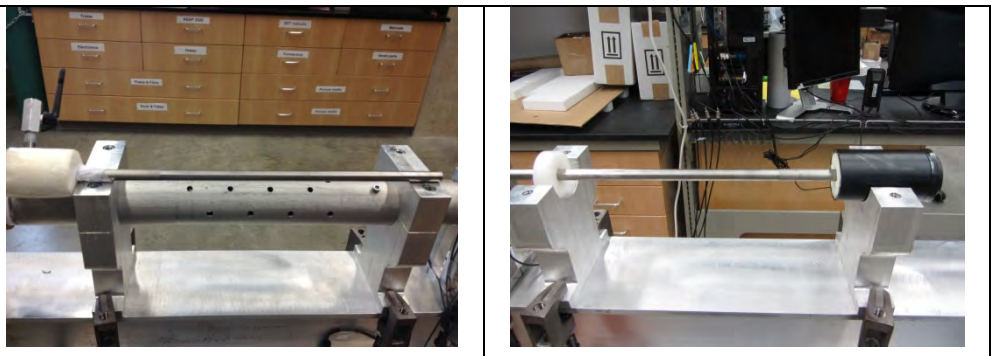

(a) The old version (b) The improved version

Fig.1.3.2 Striker holder

The quasi-static shear strength of the silica foams was less than 10 MPa, while the stress wave pressure generated by the steel striker was at least 50 MPa, at the lowest possible impact rage of about 3 m/s. A lower impact velocity is impossible, because the friction of the striker holder would prevent the striker from being projected from the gas chamber. In order to observe shear banding characteristics after testing, the extent of damage in the silica foam sample must be reasonably low. Therefore, we used a lightweight, hollow Titanium (Ti) tube striker. The striker length was 18''. It can generate stress pulses with the pressure close to 10 MPa. The PU holder, which was used to support the Ti striker in the gas chamber, helped avoid secondary impact effects related to the original Aluminum (Al) holder. A plastic secondary holder with embedded PU foam was designed and fabricated, to help precisely position the striker, the guiding holder, and the incident bar (Fig.1.3.2). In addition, the updated holder system for the Ti striker had an improved airtightness.

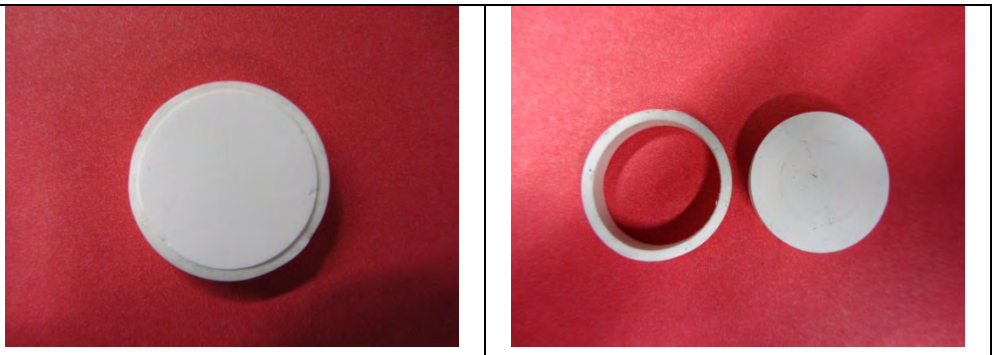

(a) Before testing (b) After testing

Fig.1.3.3 Silica foam before and after testing

1.3.2 Experimental Results and Discussion

After the dynamic shear test, the silica foam sample was only slightly damaged, with no evident

cracks, as shown in Fig.1.3.3. The impact velocity was 3 m/s.

Figure 1.3.4 shows typical wave pulses measured in the dynamic experiment. In general, the peak pressure of transmitted pulse kept decreasing as the cell size was reduced from 301 nm to 42 nm. However, when the cell size was around 152-301 nm, the relation between cell size and transmitted wave pressure was quite irregular. If the transmitted wave pressure is normalized by the incident wave pressure, the relation becomes clearer, as shown in Fig.1.3.5.

The profile seems similar with that of Fig.1.2.3(b) – This is contradictory to the concept of energy absorption. In the median range of the cell size, the quasi-static shear strength is the highest; as the foams are strong, they should absorb more stress wave energy, and, consequently, the transmitted wave pressure should be lower, conflicting with the testing data.

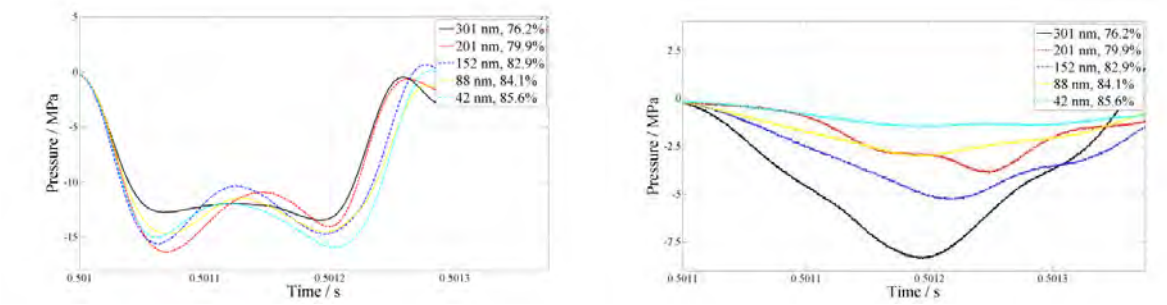

(a) Incident pulses (b)Transmitted pulses

Fig.1.3.4 Typical SHPB testing curves of silica foams
Sample thickness: 5.0 mm; Striker mass: 155.6 g; Impact speed: 3.0 m/s

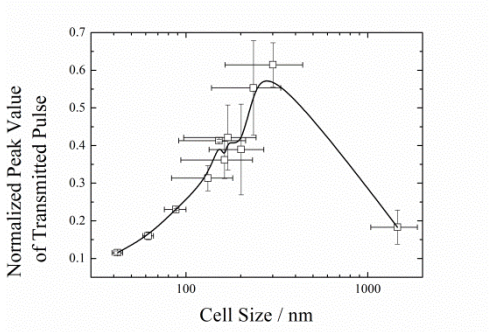

Fig.1.3.5 Normalized value of transmitted pulse.

Clearly, in addition to the quasi-static shear strength, which is dominated by porosity, there must be at least one more other mechanism that governs the energy absorption efficiency of the foam, which could be the cell size. As discussed in the previous report, as the cell size is on the nanometer scale, reducing cell size may have a beneficial effect on promoting widespread energy absorption. The competition of the two factors may lead to the complicated cell size-wave pressure relation measured in our experiment.

However, in the experiments discussed above, the influences of cell size and porosity on energy absorption could not be distinguished from each other. Better testing samples with a much narrower porosity distribution must be produced.

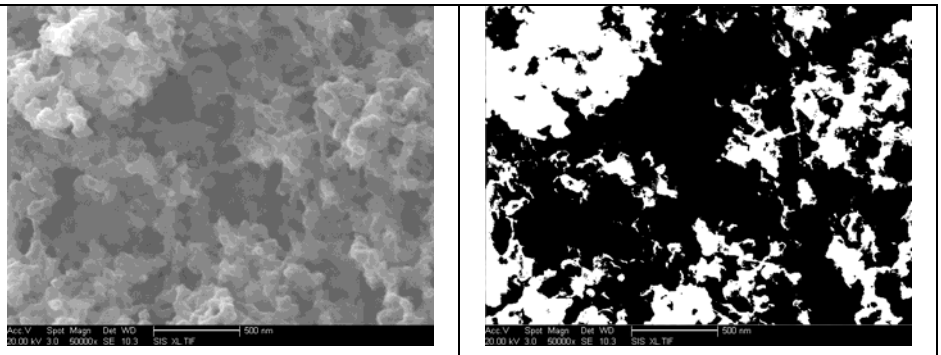

(a) Original SEM image (b) Binary image

Fig.1.4.1 Shadow in a SEM image of silica foam, without any image processing.

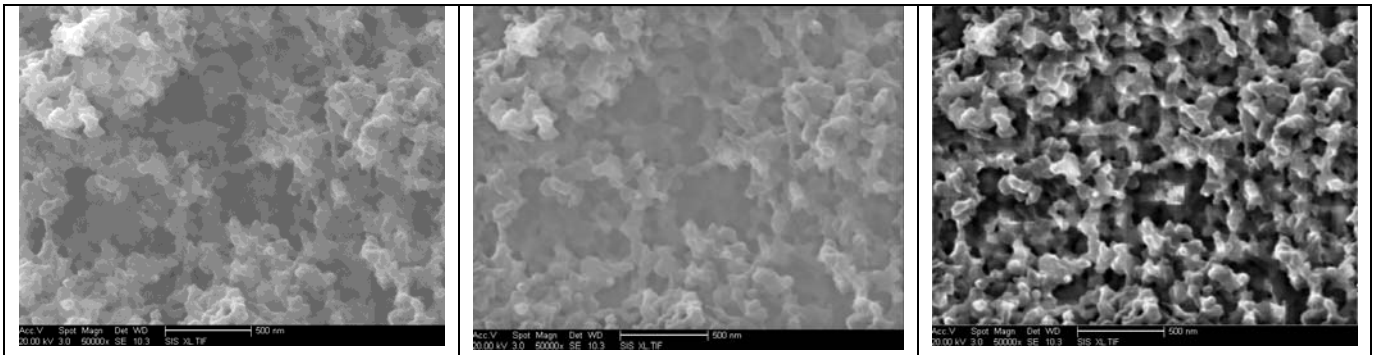

(a) Original SEM image (b) Shading-corrected image (c) Local equalized image

Fig.1.4.2 The effects of the Shadow Explosion techniques

1.4 Quantitative SEM Image Analysis

1.4.1 Development of the CalAP Technique

To precisely identify the shear bands, compression zones, and undamaged zones in tested samples, a new CalAP technique was developed, based on quantitative measurement of local porosity on SEM images:

First, a digital SEM image is treated through the Shadow Explosion (SE) process developed by us, to minimize the influence of shadow areas. The SE process is based on the Shading Correction algorithm developed by Reyes-Aldasoro, further improved by the Local Equalization

function of Image-Pro Plus. The former reduces the extent of shadow, and the latter enhances the local contrast. Typical effects are shown in Figs.1.4.1 and 1.4.2.

Second, the gray scale image is converted into a binary image. We use the Otsu's method to determine the image threshold, as shown in Figure 1.4.3.

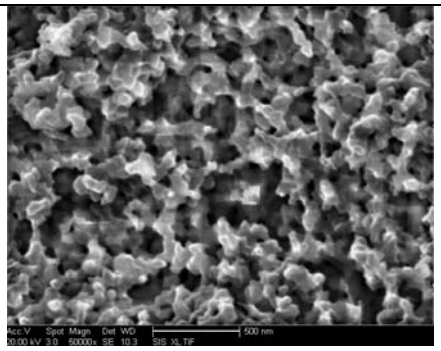

(a) Local equalized image

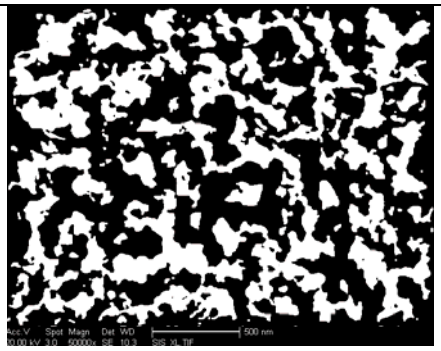

(b) Binary image

Fig.1.4.3 Image conversion from gray scale image to binary image

Third, statistical analysis is performed on a large number of SEM images. Here, a partition technique is employed to divide one image into N by N smaller ones. The local porosity is calculated as the fraction of the dark area in each local square field. The results are plotted in a 3D figure, showing the distribution of local porosity (Fig.1.4.4).

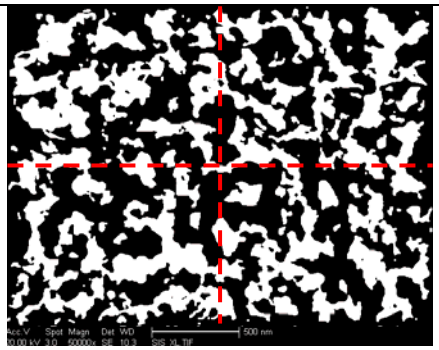

(a) Binary image

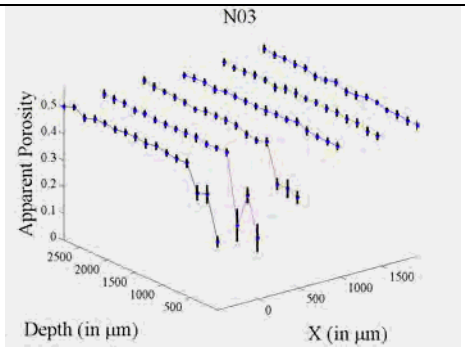

(b) Distribution of local porosity

Fig.1.4.4 Results of SEM Image Analysis

1.4.2 SEM Scanning Strategy

In order to obtain convincing results with the help of the CalAP technique, a large number of SEM images must be taken, for which we developed a SEM scanning strategy. Here we use the silica foam sample with the average cell size of 235 nm as an example to illustrate the procedure.

Step 1: Identify the scanning range of the foam sample through visual inspection. We are particularly interested in shear bands and their boundaries. As shown in Figure 1.4.5(a), the areas around the edge of the incident bar head should be scanned. Because the sections immediately adjacent to the sample-bar interface may be compressed at the beginning of the test, the far field is given a higher priority.

Step 2: Build up the X-Depth coordinate system. The origin is determined according to the characteristic surface features, shown in Figure 1.4.5 (c). The direction perpendicular to the impact direction is set as the X-direction. The X-Depth coordinate system helps locate the scanning point and coordinate the analysis results of different local fields.

Step 3: Set the scanning map. A relatively large square field ahead of the origin will be scanned. Typically, 600 images are taken for each sample, which have about 100 scan points. Usually, five or six scanning lines are needed to give an acceptable resolution of the shear band boundary. One line is for the compressed zone; one for undamaged zone; and the rest for shear band itself. About 20 points along each line are scanned. The sample thickness is 5.0 mm. To cover a half of the thickness by 20 points, the interval between them should be about 125 microns. For the sake of convenience, we set the height of each image as 186 microns at the magnification of 500X, slightly larger than the needed length (125 microns). Trivial areas may be skipped occasionally.

Step 4: Set the scanning path for each point. Location of each scanning point is critical for image analysis. The method shown in Table 1.4.1 is employed to scan each point, so that the SEM view field returns to the starting point after six images are taken.

Step 5: Take high quality SEM images for each scanning point. The scanning strategy specified in Table 1.4.1 must be strictly followed.

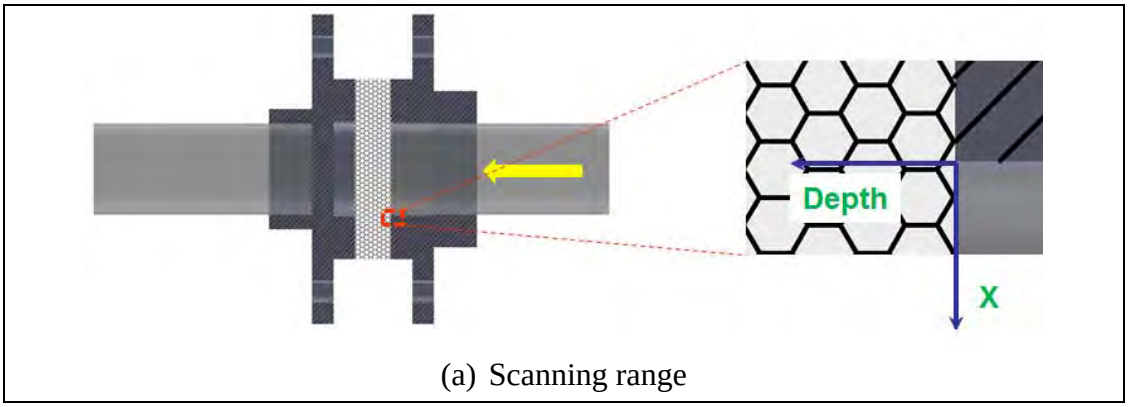

(a) Scanning range

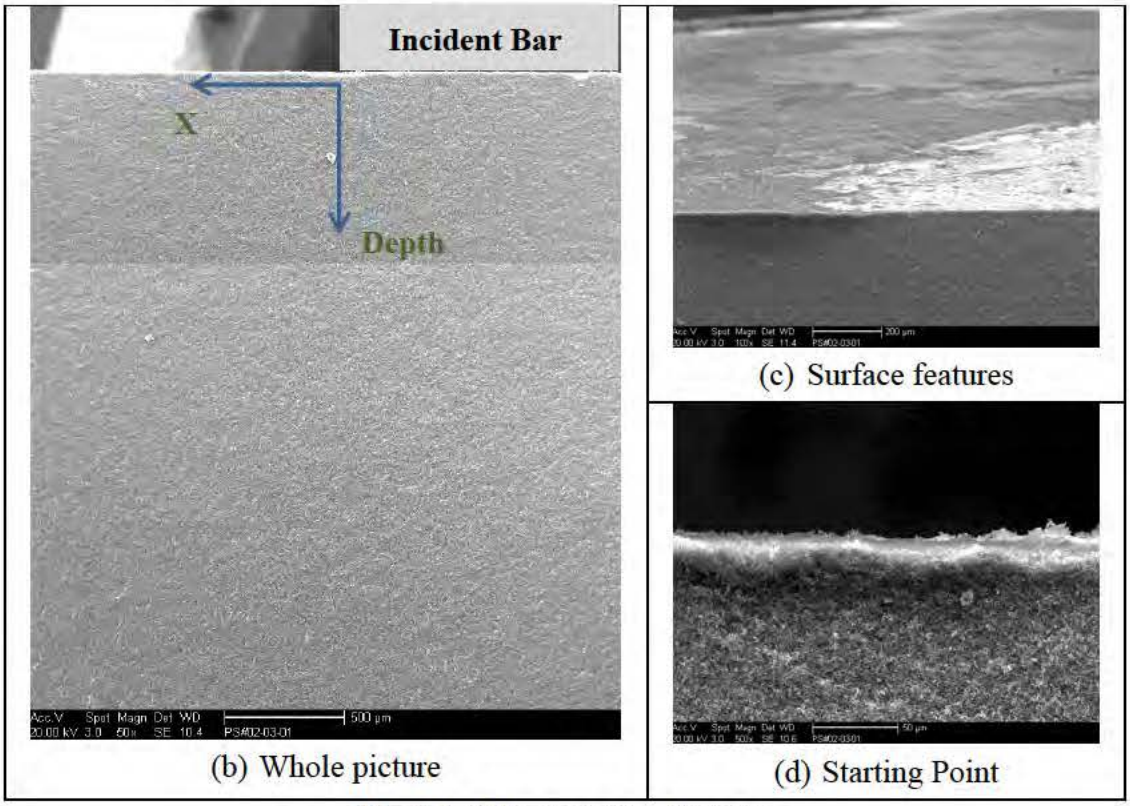

Fig.1.4.5 The scanning strategy

Table 1.4.1 SEM scanning strategy

(50 X: 242 mm×186 mm; 500 X: 242 μm×186 μm; 25000 X: 484 μm×372 μm)

	Non-compression zone				Starting Point			Compression zone
X / Depth	968	726	484	242	0			-242
0					5	4	3	
					6	1	2	
186								
372								
558								
744								

1.4.3 Image Analysis

Using the CalAP technique, we measured the distribution of local porosity for selected samples, and determined the shear band boundaries. Here, we take the silica foam sample with the cell size of 235 nm as an example to show the image analysis procedure:

The partition number of each SEM image is set as 3 by 3. The analysis results are listed in Table 1.4.2. Six lines are scanned; each line covers a half of the sample thickness. The areas (points)

close to the origin tend to have smaller local porosity. An interesting observation is that the bucked zones may not be continuous.

Table 1.4.2 Results of Image Analysis
Cell size 235 nm; Porosity 78.8%; Partition 3X3; Critical value 0.468

:	X										
on	968	Stdev	726	Stdev	484	Stdev	242	Stdev	0	Stdev	-242
0	0.4625	0.0145	0.4601	0.014	0.4562	0.0172	0.4618	0.0138	0.4665	0.0114	0.4693
186	0.472	0.0171	0.469	0.0149	0.4719	0.011	0.46	0.0118	0.4696	0.0134	0.4759
372	0.4688	0.0153	0.4683	0.0146	0.4739	0.0126	0.4685	0.0111	0.4646	0.0136	0.4709
558	0.4761	0.0149	0.4748	0.0147	0.471	0.0127	0.4655	0.0177	0.4692	0.0194	0.4767
744	0.4764	0.0121	0.4708	0.0161	0.4773	0.0148	0.4617	0.0155	0.4805	0.012	0.4645
930	0.4695	0.0151	0.4695	0.0167	0.4768	0.0172	0.4779	0.0147	0.4694	0.0129	0.464
1116	0.4647	0.0118	0.4768	0.0147	0.4723	0.0171	0.4716	0.0189	0.4688	0.0121	0.4675
1302	0.4727	0.0128	0.471	0.0176	0.4758	0.0176	0.4791	0.0171	0.4777	0.015	0.4754
1488	0.4639	0.0156	0.4671	0.0143	0.4606	0.013	0.4717	0.0129	0.4606	0.0125	0.4756
1674	0.4715	0.0152	0.4734	0.0186	0.4637	0.0177	0.4754	0.0146	0.4767	0.011	0.471
1860	0.4701	0.0163	0.4689	0.0184	0.4813	0.0171	0.4748	0.0193	0.4616	0.0137	0.4772
2046	0.4727	0.0161	0.4671	0.0163	0.4747	0.0213	0.488	0.014	0.4801	0.013	0.4786
2232	0.4717	0.0147	0.4802	0.0112	0.4737	0.0153	0.4786	0.0205	0.468	0.0167	0.4689
2418	0.4774	0.0184	0.4732	0.0125	0.4669	0.0177	0.4787	0.0169	0.474	0.0165	0.4831

Table 1.4.3 Updated Results of Image Analysis
Cell size 235 nm; Porosity 78.8%; Partition 3X3; Background porosity: 0.4754; Threshold 0.983

Unit: Micron	X					
	968	726	484	242	0	-242
0	0.9728	0.9678	0.9596	0.9714	0.9812	0.9871
186	0.9928	0.9865	0.9926	0.9676	0.9878	1.001
372	0.9861	0.985	0.9968	0.9855	0.9773	0.9905
558	1.0014	0.9987	0.9907	0.9791	0.9869	1.0027
744	1.0021	0.9903	1.004	0.9712	1.0107	0.977
930	0.9876	0.9876	1.0029	1.0052	0.9873	0.976
1116	0.9775	1.0029	0.9934	0.992	0.9861	0.9834
1302	0.9943	0.9907	1.0008	1.0078	1.0048	1
1488	0.9758	0.9825	0.9688	0.9922	0.9688	1.0004
1674	0.9918	0.9958	0.9754	1	1.0027	0.9907
1860	0.9888	0.9863	1.0124	0.9987	0.9709	1.0038
2046	0.9943	0.9825	0.9985	1.0265	1.0099	1.0067
2232	0.9922	1.0101	0.9964	1.0067	0.9844	0.9863
2418	1.0042	0.9953	0.9821	1.0069	0.997	1.0162

Depth

We assume that (a) The cells along the line of X=0 undergo the largest deformation; and (b) Buckeling is less pronounced in the far field. Based on these two assumptions, a critical local porosity, normalized by the porosity in undamaged zone, of 0.468 is selected to define the shear

band boundary. For instance, the background porosity for silica foam with the average cell size of 235 nm is 0.4754. Table 1.4.3 gives the updated analysis results. As criterion is set to 0.983, the shear band boundary is marked by the red numbers.

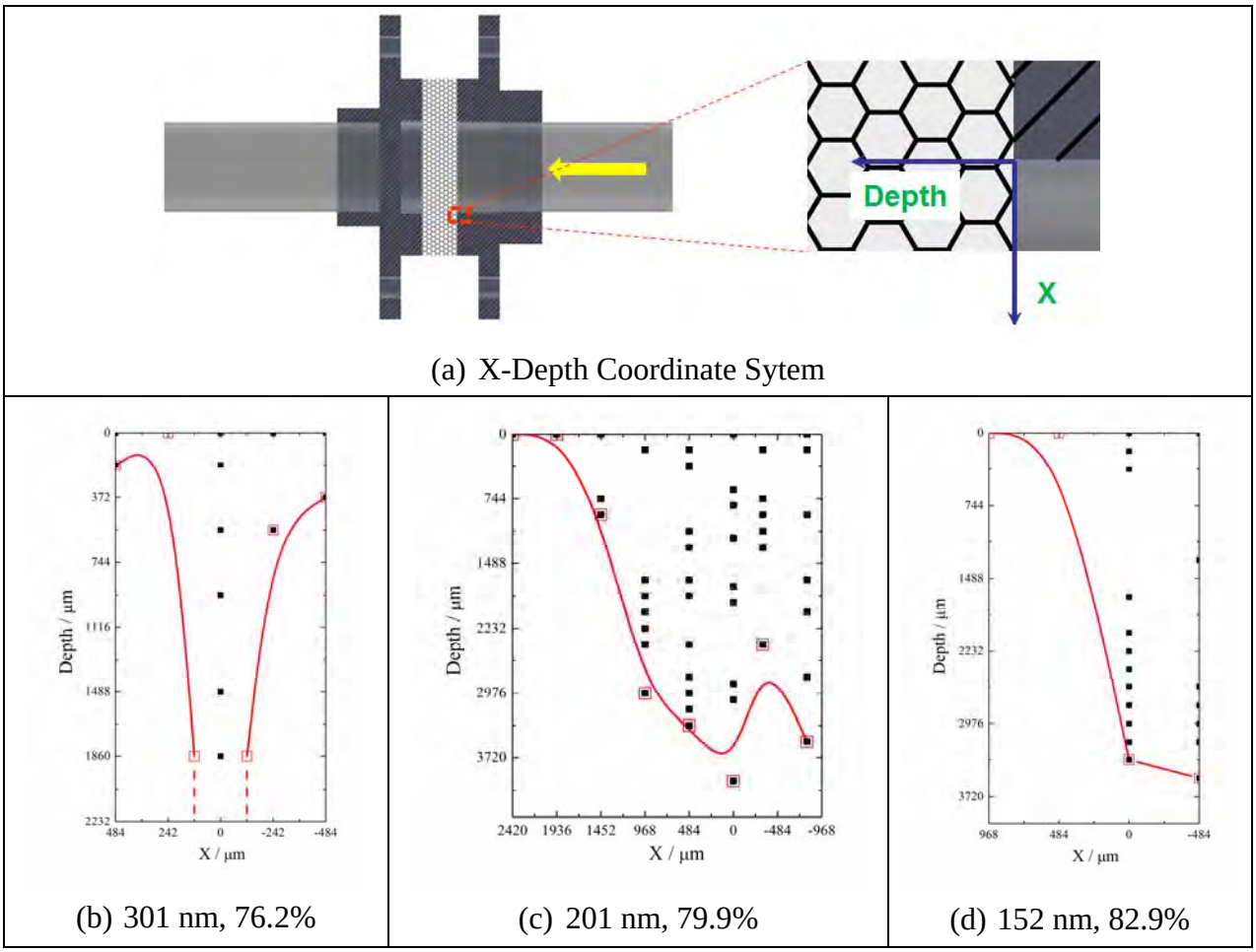

(a) X-Depth Coordinate Sytem

(b) 301 nm, 76.2%

(c) 201 nm, 79.9%

(d) 152 nm, 82.9%

Fig.1.4.6 Cell-buckling zone

Sample thickness 5.0 mm; Impact speed of striker 3.0 m/s; Criterion of image analysis 0.983

1.4.4 Shear Band Zones

In Figure 1.4.6, the profiles of shear bands in silica foams of various average cell sizes are depicted. Compressed zones are indicated by black squares; shear boundary boundaries are indicated by red squares. When the average cell size is 301 nm, a narrow band can be clearly seen. When the cell size is 201 or 152 nm, the damaged area becomes much broader. Apparently, reducing cell size has a beneficial effect on promoting widespread energy absorption.

Table 1.4.4 shows the relationship between the pressure reduction of transmitted wave and the

shear band width. The silica foam with the average cell size of 201 nm exhibits the most intensive cell buckeling, leading to the largest pressure reduction. However, due to the influence of porosity, the data scatter is quite large, making the results somewhat non-conclusive.

Table 1.4.4 Combined SEM images with cell-buckling zone marked
(Total mass of Ti striker 155.6g; Impact speed of striker 3.0 m/s)

(a)	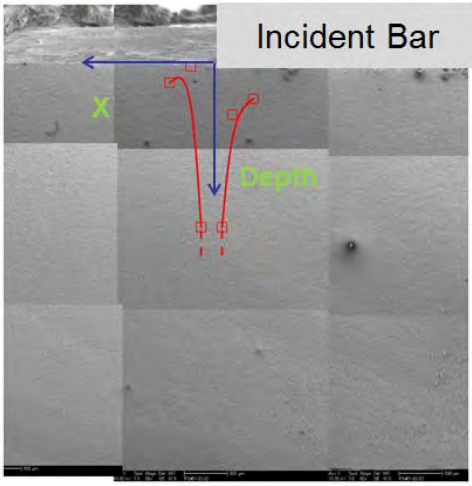	**Sample Information** Average cell size: 301 nm Porosity: 76.1% Static shearing pressure: 9.33 MPa Dimensions: D19.40 mm, T5.02 mm Criterion of image analysis: 98.3% **Dynamic Shearing Results** Average incident pulse: 12.08MPa Peak value of transmission pulse: 8.37MPa Normalized peak value: 0.693 Pressure reduction: 0.96 MPa
(b)	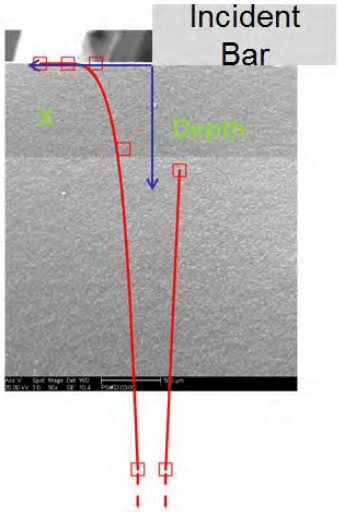	**Sample Information** Average cell size: 235 nm Porosity: 78.8% Static shearing pressure: 9.21 MPa Dimensions: D19.98 mm, T5.02 mm Criterion of image analysis: 98.3% **Testing Results** Average incident pulse: 10.73MPa Peak value of transmission pulse: 7.93MPa Normalized peak value: 0.739 Pressure reduction: 1.28 MPa

(c)	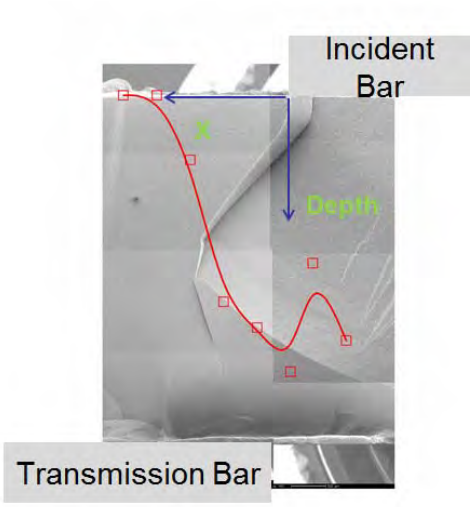	**Sample Information** Average cell size: 201 nm Porosity: 80.0% Static shearing pressure: 9.95 MPa Dimensions: D20.75 mm, T5.02 mm Criterion of image analysis: 98.3% **Testing Results** Average incident pulse: 12.89MPa Peak value of transmission pulse: 3.92MPa Normalized peak value: 0.304 Pressure reduction: 5.93 MPa
(d)	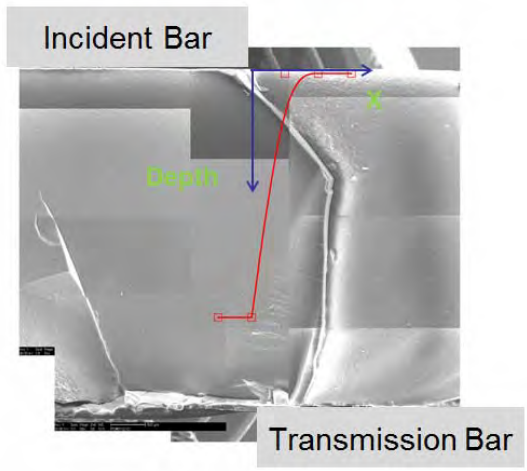	**Sample Information** Average cell size: 163 nm Porosity: 82.5% Static shearing pressure: 5.34 MPa Dimensions: D22.06 mm, T5.05 mm Criterion of image analysis: 98.3% **Testing Results** Average incident pulse: 13.21MPa Peak value of transmission pulse: 4.32MPa Normalized peak value: 0.327 Pressure reduction: 1.02 MPa
(e)	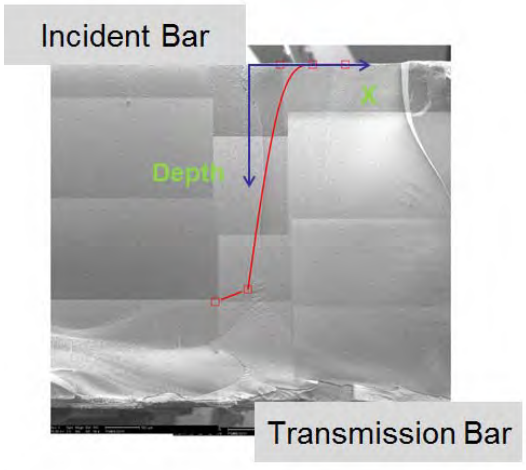	**Sample Information** Average cell size: 152 nm Porosity: 82.9% Static shearing pressure: 5.34 MPa Dimensions: D22.40 mm, T5.05 mm Criterion of image analysis: 98.3% **Testing Results** Average incident pulse: 12.98MPa Peak value of transmission pulse: 5.32MPa Normalized peak value: **0.410** Pressure reduction: 0.02 MPa

2. SINGLE-PARAMETER STUDY ON SILICA FOAMS

Thus, we developed a set of new approaches to conduct single-parameter study on silica foams. The goal is to minimize the variation in porosity, so that different samples have only one major variable – the cell size.

2.1 Precise Control of Porosity

Among the large number of key processing parameters, the sintering (curing) temperature of silica gel was identified as a critical factor for precise control of porosity, with little detrimental effect on cell size adjustment. To minimize the distribution of quasi-static shear strength of silica foams of different cell sizes, the porosity must be within a narrow range, for which the treatment temperature was nearly constant, leading to stable Young's moduli. Typically, the silica foam samples were treated at the target temperature for 1 hour. The ramp rate was set to 3 °C /min first when the temperature was more than 100°C lower than the target temperature, and then 1 °C /min to avoid the potential overshooting. The results are listed in Table 2.1.1.

Table 2.1.1 Results of tuning porosity via using various temperature

Sample No.	Temperature / °C	Diameter / mm	Porosity	Cell Size / nm
#03	850	20.82	85.6%	210±67
#03	1250	17.45	55.1%	159±70
#07	850	22.98	83.8%	132±49
#07	1250	17.55	65.8%	106±41
#10	850	24.67	79.9%	41±3
#10	1150	22.82	78.1%	44±2
#10	1200	21.49	76.0%	45±7
#10	1250	16.96	65.5%	46±9

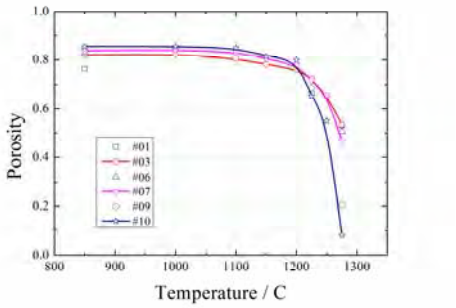

Fig.2.1.1 Relationship between the final porosity and the target temperature. The curve is affected by the initial sample size.

2.1.1 Porosity vs. Curing Temperature

As shown in Figure 2.1.1, there is no evident variation in porosity when the target temperature is lower than 1,100 °C. The cell structure begins to shrink dramatically when the temperature reaches a critical value corresponding to a threshold cell size. In general, a silica foam with a smaller cell size prefers a lower sintering temperature, due to its larger surface area. To obtain the porosity of 60%, the target temperature should be set to 1235-1270 °C.

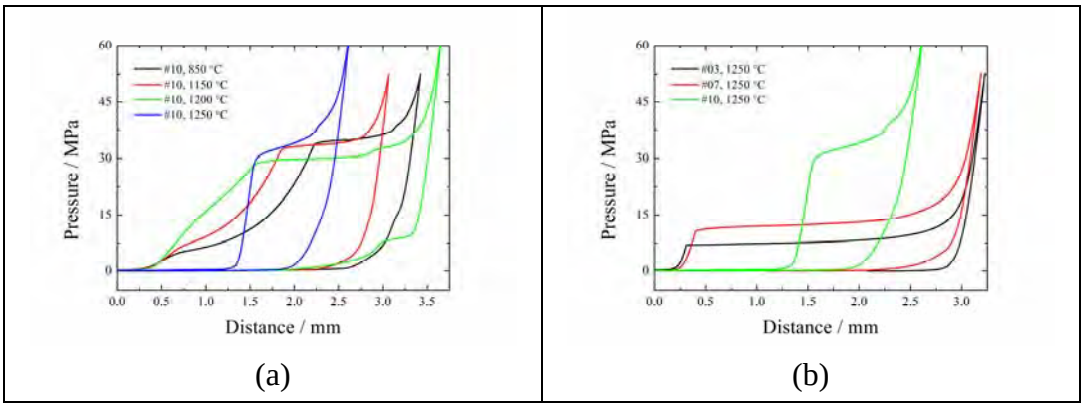

Fig.2.1.2 Results of mercury porosimetry. The sample size was not normalized. The cell size is indicated by the height of the infiltration plateau.

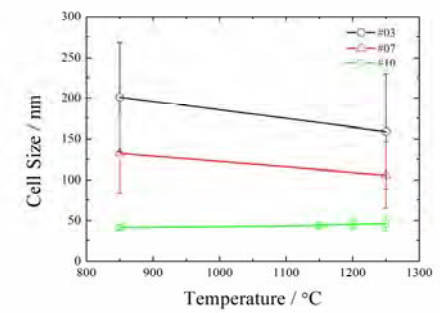

Fig.2.1.3 Relationship between the cell size and the curing temperature

2.1.2 Cell Size vs. Curing Temperature

The mercury porosimetry data of silica foams cured at different temperatures were given in Figure 2.1.2. The relatively flat plateau indicates a relatively narrow cell size distribution. Note that the low-pressure plateaus in some curves, e.g. sample #10 of a low curing temperature of 850 °C, does not reflect the acutal cell size distribution, as it is related to the low sample strength. The actual cell size distribution should be obtained by using the method shown in Figure 1.1.3(b). From Figure 2.1.3, we can see the trend that after being treated at a higher temperature, large cells tend to shrink while smaller cells tend to expand. Compared with the porosity, the

temperature has a much less influence on the cell size, suggesting a possible approach to uncouple the porosity and the cell size (Figure 1.2.2b), attractive for our one-parameter study.

2.1.3 Design of Curing Molds

As depicted in Figure 1.3.2, the incident bar has a diameter of 12.7 mm. To promote shear bands in a silica foam disk sample with the shear-promoting holder (ISPH), the diameter of the sample should be much larger. The old curing mold is relatively small, leading to a final sample diameter, with a target porosity of 60% and the curing temperature range of 1235-1270 °C, less than 17 mm, insufficient for accurate measurement and observation of shear banding phenomena. Therefore, the size silica foam sample must be increased.

Figure 2.1.4 gives the relationship between the porosity and the final diameter of cured silica foams, which guides the design of curing mold. The normalized diameter is defined as the ratio between the absolute diameter of the sample to the diameter of the curing mold. Taking the foam sample with the porosity of 60% as an example, the normalized diameter is within the range of 0.65-0.70, implying that the curing mold should have a diameter of 31-34 mm, if the target final sample diameter is 22 mm.

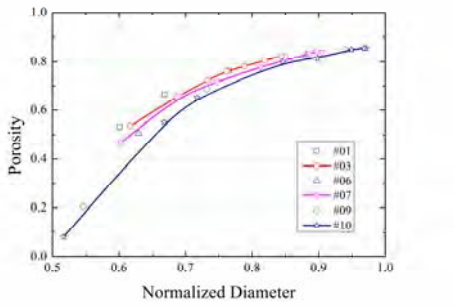

Fig.2.1.4 Relationship between porosity and diameter of the silica foam

2.2 Characterization of Large-Sized One-Parameter Silica Foams

Large-sized silica foams were synthesized by carefully controlling the curing temperature and using molds with diameters of 35.6 mm. After curing at temperature within the range of 1235-1270 °C for one hour, the density and the cell size range of the sample were measured through the same procedures as described Section 1.1. The results are listed in Table 2.2.1. The diameters of the silica foam disks are larger than 22 mm, sufficient to avoid boundary effects during SHB testing. The density was controlled with the range of 0.81-0.91 g/cm^3, so that the samples, regardless of their cell sizes, have nearly the same quasi-static shear strengths. The average cell size varies from 47 nm to 1049 nm by more than one order of magnitude, well covering the

critical range around 200 nm identified in the two-parameter study. The porosity distributes in a relatively narrow range from 58.5% to 63.2 %, with the average porosity around 61% and the variation less than 3.5% of the average value.

Table 2.3.1 Quasi-static shear strength of silica foams
(Sample thickness: 4.50 mm; Loading rate: 0.01 mm/min; Shear depth: 0.5 mm)

Sample No.	Porosity	Cell Size / nm	Static Shearing Strength / MPa
1	61.5%	1049±459	10.80
2	63.8%	271±137	12.71
3	60.0%	213±110	11.69
4	60.1%	163±68	10.47
5	57.4%	144±55	9.78
6	60.5%	109±37	10.78
7	60.6%	83±24	8.93
8	55.8%	62±15	14.57
9	61.8%	47±10	12.04

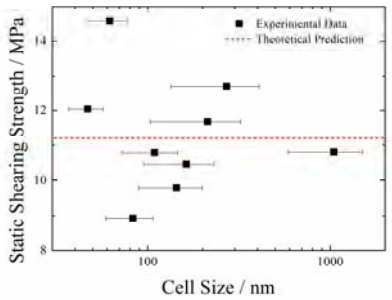

Fig.2.3.1 Static shearing strength of silica foam with porosity ~61%
Sample thickness: 4.50 mm; Loading rate: 0.01 mm/min

2.3 Quasi-Static Shear Testing on One-Parameter Silica Foam Samples

The results of quasi-static shear testing on the one-parameter silica foams are listed in Table 2.3.1 and Figure 2.3.1. We can clearly see that the quasi-static shear strength varies in a relatively narrow range around the theoretical value, 11.2 MPa, and there is no evident correlation between the strength and the cell size.

2.4 SHPB Dynamic Testing

With the improvement in the quality of one-parameter silica foams, particularly the increase in strength, the impact rate of SHPB test was raised to 8.5 m/s, compared to 3 m/s for the two-parameter samples. The higher impact rate, however, impose tougher requirements on the

polyurethane (PU) holders of the Titanium (Ti) striker. Therefore, a much harder PU holder was used, and fibrous separation layers were inserted between the PU holder and the striker, so as to avoid secondary impact effect.

2.4.1 Experimental Data

Using the improved SHPB system with the reinforced PU holder, complete single-pulse signals were successfully measured for the one-parameter silica foam samples. Figure 2.4.1 shows the typical testing curves for a sample, with the impact speed of 8.5 m/s.

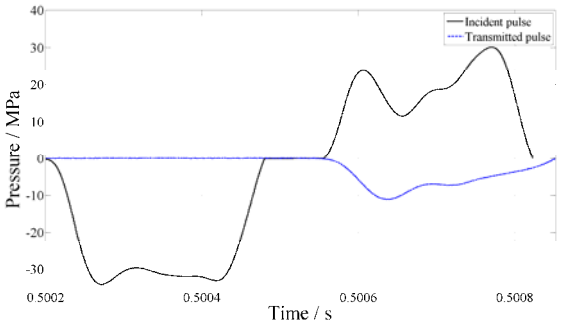

Fig.2.4.1 Typical SHPB Measurement Curves for a Silica Foam
Cell size 163 nm; Porosity 60.3%; Sample thickness 4.50 mm; Impact speed 8.5 m/s

Data of silica foams with different average cell sizes were given in Figure 2.4.2. The incident wave pressure was nearly the same for all the samples, around 33 MPa. There is a consistent reduction in transmitted wave pressure, P_t, with the decrease in cell size. Particularly, there is a transition zone around 100-200 nm, as shown in Fig.2.4.3. Above this cell size range, from 200 nm to more than 1 μm, the transmitted wave pressure (P_t) is relatively high, and as the cell size increases, P_t rises only slightly – Note that the horizontal axis in Fig.2.4.3 is on log scale. When the cell size is reduced from above 200 nm to below 100 nm, P_t rapidly decreases from about 18 MPa to about 11 MPa, by nearly 2/3. Below 100 nm, the transmitted wave pressure becomes insensitive to further reduction in cell size.

An interesting coincident is, as the cell size is below 100 nm, the lower plateau of the transmitted wave pressure is around 11 MPa, quite close to the quasi-static shear strength of the foams (σ_b). That is, the energy absorption capacity of the foam sample is fully utilized: When the wave pressure is lower than the foam strength, no energy absorption mechanism can be activated, and, therefore, P_t can never be lower than σ_b. With the increase in cell size, apparently the energy absorption efficiency is reduced, so that the pressure of transmitted wave rises to above σ_b.

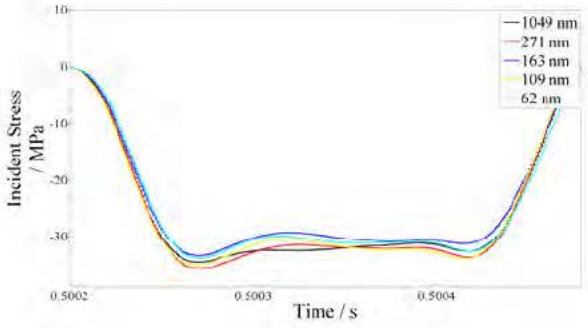

(a)

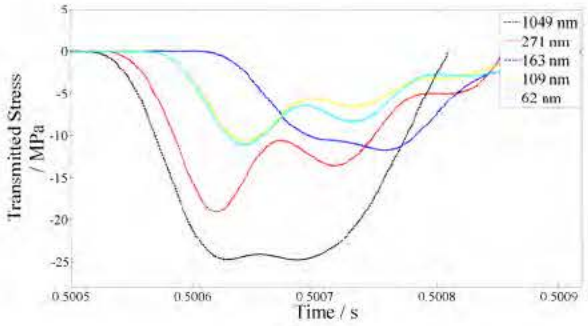

(b)

Fig.2.4.2 Typical SHPB Curves: (a) Incident waves and (b) Transmitted waves
Porosity 60.3%; Sample thickness 4.50 mm; Impact speed 8.5 m/s

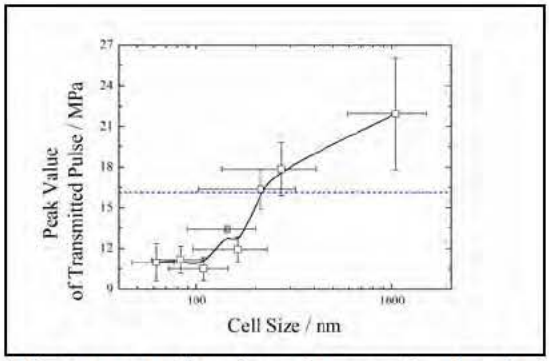

Fig.2.4.3 Peak value of transmitted pulse
Porosity: 60.3%; Sample thickness: 4.50 mm; Impact speed: 8.5 m/s

2.4.2 Assessment of Absorbed Energy

The output energy carried by the transmitted wave is assessed, as shown in Fig.2.4.4, which exhibits the same trend as the transmitted wave pressure. We defined

Where U_{in}, U_{re} and U_{tr} are the total energy carried by the incident, reflected and transmitted pulses, respectively, which accounts for both the strain energy and the kinetic energy. For a given pulse (pressure-time curve), the carried total energy is calculated as

$$U = U_0 + U_k = \xi \int_0^T \sigma^2(t)dt$$

where ξ is a system constant, T is the pulse duration, $\sigma(t)$ is the pulse pressure, and t indicates time. A smaller value of α corresponds to a higher energy absorption efficiency. Again, the results suggests that reducing cell size to below 100-200 nm has a consistent, beneficial effect on increasing energy absorption efficiency.

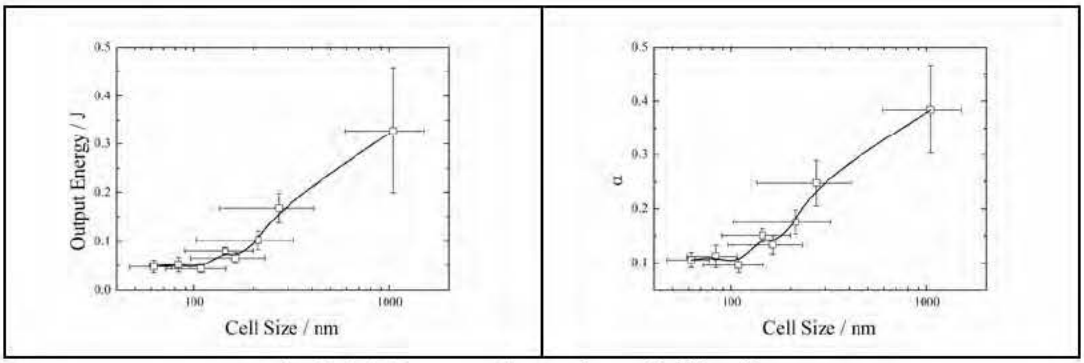

Fig.2.4.4 Energy absorption of silica foams
Porosity: 60.3%; Sample thickness: 4.50 mm; Impact speed: 8.5 m/s

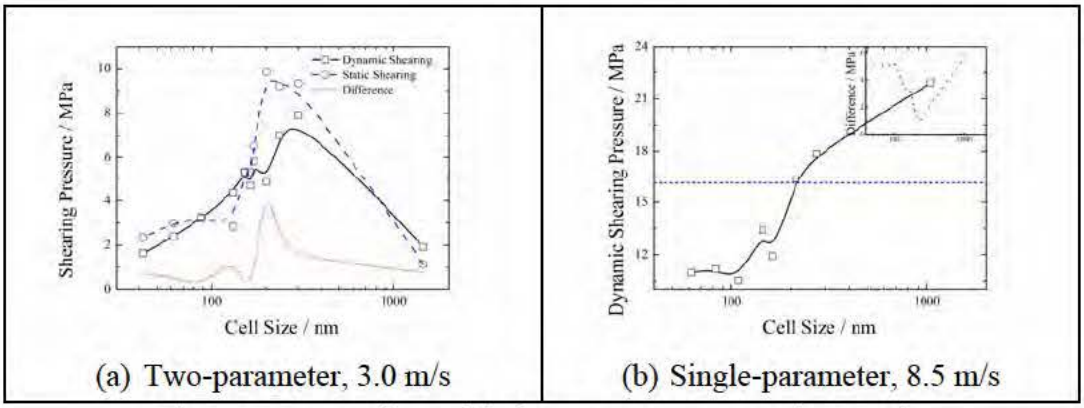

(a) Two-parameter, 3.0 m/s (b) Single-parameter, 8.5 m/s

Fig.2.4.5 Comparison with the two-parameter testing results

2.4.3 Comparison with the Two-Parameter Testing Results

Figure 2.4.5 compares the results of the previous two-parameter testing and the single-parameter testing. It can be seen that the one-parameter testing data are more conclusive, as the influence of porosity is minimized. The transmitted wave pressure is mainly affected by the cell size. Nevertheless, in both tests, there is a transition zone around 100-200 nm.

2.4.4 On-going SEM Image Analysis

SEM image analysis is currently on going. The preliminary results showed encouraging evidence that, as the cell size is reduced from above 200 nm to below 100 nm, widespread cell buckling is promoted, consistent with the observation of transmitted wave pressure and energy. Figure 2.4.6 shows a few examples. Figure 2.4.7 shows the preliminary results of boundaries of cell buckling zones. As the cell size is above 200 nm, a narrow shear band can be clear seen, depicted by the dashed-dot line; as the cell size is reduced, the cell deformation zone is significantly broadened, suggesting that widespread energy absorption is promoted. This work is still incomplete. We are collecting information from more SEM images.

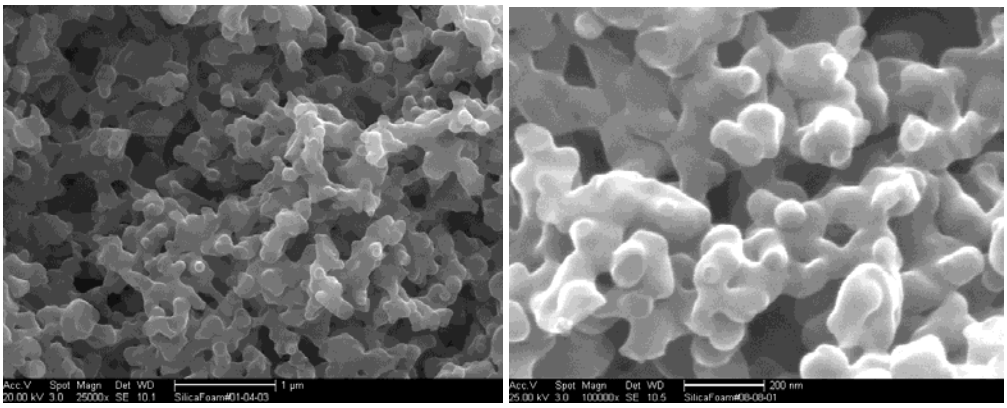

Figure 2.4.6 Samples with average cell sizes of 271 nm (left) and 144 nm (right).

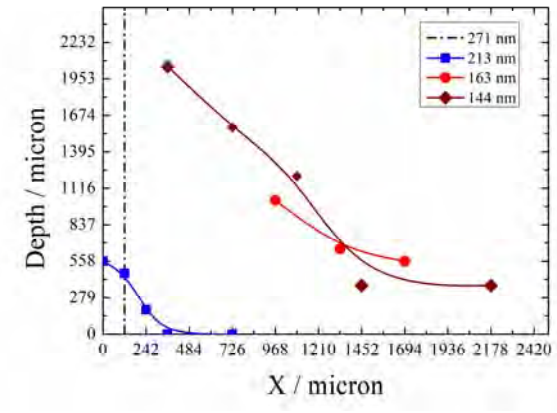

Figure 2.4.7 Measurement results of boundaries of cell buckling zones.
This work is still incomplete

3. CONCLUDING REMARKS AND FUTURE WORK

We have successfully processed, characterized, and tested one-parameter silica foams, and concluded that

1) In all the one-parameter silica foam samples, the porosity is nearly constant, around 61%; the average cell size ranges from tens of nm to a few μm.
2) SHB testing clearly demonstrates that as the cell size is reduced from above 200 nm to below 100 nm, the transmitted wave pressure and energy are significantly lowered, suggesting that the energy absorption efficiency is enhanced.
3) When the cell size is larger than 200 nm or smaller than 100 nm, its effects on transmitted wave pressure and energy are secondary, converging to the behaviors of conventional porous materials.
4) SEM analysis of single-parameter samples is on going, and the preliminary results are encouraging.

In the following period of performance, we plan to

1) Complete SEM analysis on single-parameter silica nanofoam samples.
2) Complete data analysis for single-parameter silica nanofoam samples.
3) If possible, conduct drop tower tests on single-parameter silica nanofoam samples.
4) If possible, investigate polymer and/or metallic nanofoam samples.
5) If possible, investigate functionally graded nanofoams.
6) If possible, investigate nanofoam matrix, fiber reinforced composites.